

Review for publication in shock and vibration

Active controller design for microgravity isolation systems

Nan-Chyuan Tsai

Mechanical Engineering Department, Southern Taiwan University of Technology, Tainan 710, Taiwan
Tel.: +886 6 2533131 ext. 3530; Fax: +886 6 2426154; E-mail: ntsai@ms42.hinet.net

Received 4 December 2000

Revised 5 January 2002

Abstract. This paper examines the performance of active isolation systems for microgravity space experiments as a function of desired transmissibilities that are chosen to be either much below or close to what can be tolerated. The control system utilizes two feedback signals: absolute acceleration and relative displacement of the controlled mass. The controller transfer function for acceleration feedback is chosen to avoid marginally stable pole-zero cancellations. The controller transfer function for relative displacement feedback is determined to achieve the desired transmissibility function. The issue of stability and properness of this controller transfer function are discussed. The required input forces and equivalent closed-loop stiffness are examined for various examples of desired transmissibilities.

Keywords: Microgravity, transmissibility, transfer function

1. Introduction

The acceleration levels required for microgravity science experiments are expected to be much smaller than what will be found on a space station. The microgravity isolation systems are inherently multivariable with inertia coupling in dynamics, uncertainty and nonlinearities. Grodinsky and Whorton [7] reported a detailed survey and related discussions. Therefore, a number of researchers are working on the development of active control systems to ensure a proper acceleration environment [9,10,17]. Jones et al. have presented a conservative estimate of the frequency spectrum of acceleration levels found on a spacecraft (Fig. 1). In space stations, the frequency spectrum of acceleration levels required for many experiments is also shown in Fig. 1. This spectrum was presented by Columbus Attached Laboratory and Columbus Free-Flying Laboratory in European Space Research and Technology Centre, Netherlands, under the potential excitation environment mainly caused by gravity gradient, air drag,

crew motion and machine rotating [16]. On the basis of these curves, the required acceleration transmissibility for a vibration isolation system has been obtained (Fig. 2). This paper deals with the performance of control systems designed to achieve transmissibility functions that are either much below or close to the desired transmissibility specified in Fig. 2.

Jones et al. [10] have developed an active microgravity isolation mount using a Lorentz type of electromagnetic actuator. Their controller is based on the classical phase lead/lag compensator and utilizes the displacement of the mass relative to the base as feedback signal because the absolute displacement of the controlled mass cannot be directly measured. Jones et al. [11] reported the development of a microgravity isolation mount that will be accommodated within the standard rack of system at Columbus laboratories. Stampleman and Von Flotow [12] have established a semi-active isolation mount using piezoelectric film. Fenn et al. [3] have developed an active isolation system using Lorentz type of electromagnetic actuator and

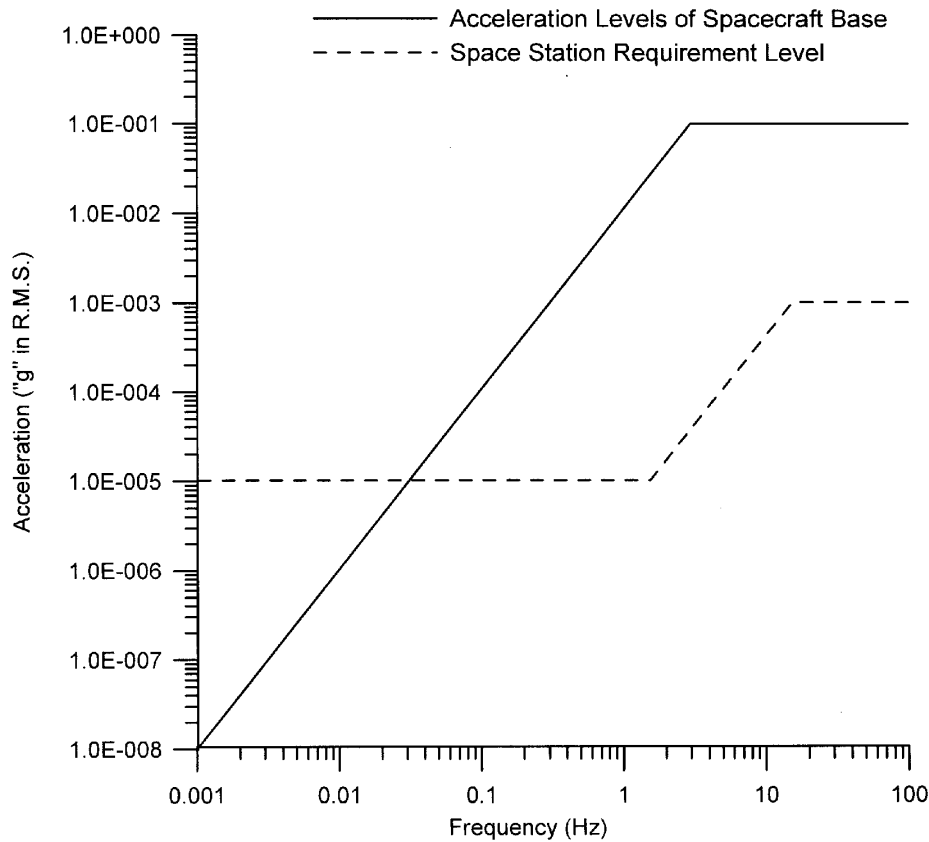


Fig. 1. Estimated acceleration levels on space station.

nonlinear control law. At NASA Lewis Research Center, an active isolation system has been developed [5, 6]. In addition to using relative displacement signal, base acceleration is measured and integrated to achieve the feedback of the absolute velocity.

In all the cited papers, system transmissibility can be obtained to be close to the desired level by appropriately tuning the controller parameters. However, it is not a straightforward task to achieve the desired performance and resulting transmissibilities do exceed the desired values in many cases. Consequently, Sinha and Kao [13] and Tsai and Sinha [15] have developed a methodology to determine the controller transfer functions that will perform much below or exactly achieve the desired transmissibility. The formulation has been developed to incorporate relative displacement and absolute acceleration of the mass as feedback signals. As an important example, the desired transmissibility was chosen to be $1/(\tau s + 1)^2$ where $1/\tau = 0.03$ Hz. The frequency spectrum of this transfer function is evidently below the specified transmissibility. The controller obtained using the new approach has also been

found to require input force which is smaller than that required by the classical phase lead/lag approach. Tsai and Sinha [15] also found a marginally stable pole-zero cancellation for the control system with relative displacement feedback only. Therefore, an analog inner feedback loop has been added by utilizing the absolute acceleration signal. Meanwhile, a digital algorithm to achieve the desired transmissibility corresponding to $1/(\tau s + 1)^2$ has been established by Sinha and Wang [14].

The choice of $1/(\tau s + 1)^2$ as the desired transmissibility does lead to an acceptable performance in terms of transmissibility. In fact, the resulting transmissibility is much less than what can be tolerated at high frequencies. The response of the closed-loop system to a direct force excitation on the mass and required input levels are also important considerations in the design of an isolation system. Therefore, the following issue arises: is there a better choice of desired transmissibility function which will satisfy the transmissibility requirement and at the same time has a superior performance in terms of required input and the sensitivity

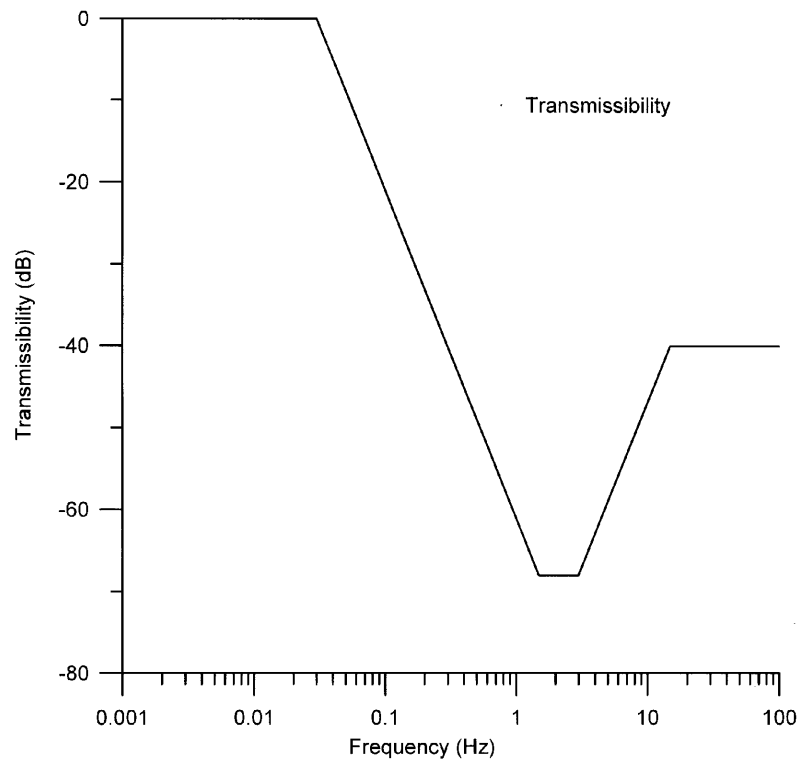


Fig. 2. Desired transmissibility.

to direct force excitation? To explore this issue, a controller is firstly designed using relative displacement feedback such that the transmissibility is close to the specified function over the complete frequency spectrum (Fig. 2). It is also found that an absolute acceleration feedback loop has to be used to avoid undesired pole-zero cancellations. Furthermore, a factor $(s + \alpha)^2$ has to be added to the denominator of the desired transmissibility function in order to obtain a proper controller transfer function. If α is properly chosen, the desired transmissibility will exactly match the specified transmissibility in the frequency range of interest. On the other hand, the resulting transmissibility can also be made very conservative by choosing a smaller value of α . The equivalent closed-loop stiffnesses of isolation systems for transmissibility function $1/(\tau s + 1)^2$ (CASE I) and transmissibility function corresponding to Fig. 2 with a variable α (CASE II) are examined by considering the unit step response. Because of the acceleration feedback loop, the steady state responses for both cases are found to be zero. Therefore, the maximum displacement of the mass has been taken to be a measure of the equivalent closed-loop stiffness. That is, the higher the maximum displacement, the smaller is the equivalent closed-loop stiffness. Input forces for

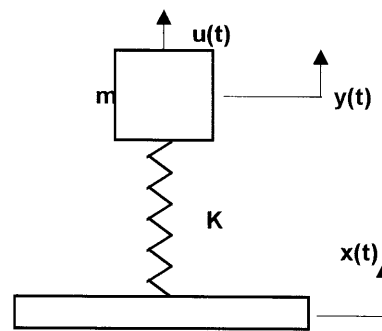


Fig. 3. Mass-spring model experiment module.

all designs have been evaluated and compared for both cases.

2. System model

Consider the single degree of freedom system shown in Fig. 3 where m and k are the mass of the experiment module and the umbilical stiffness, respectively. The umbilical stiffness k represents the connections between the experiment module and the base, which are necessary for various functions such as the supply

for electric power, the transport of the cooling fluid, etc. The base acceleration $\ddot{x}(t)$ represents the acceleration of the spacecraft or the space station.

The differential equation of motion for the system shown in Fig. 3 can be described as follows:

$$m\ddot{y}(t) + k[y(t) - x(t)] = u(t) \quad (1)$$

where $u(t)$ is the control force.

In the absence of any control force, i.e., $u(t) = 0$, the transmissibility $G_p(s)$ is defined and obtained as follows:

$$G_p(s) = \frac{Y(s)}{X(s)} = \frac{k}{ms^2 + k} \quad (2)$$

3. Desired transmissibility functions

The objective of this paper is to design a feedback control system such that the transmissibility of the closed-loop system is close to or below the desired function shown in Fig. 1. Two cases of the desired transmissibility functions are discussed as follows:

3.1. CASE I:

Sinha et al. [13] have taken the following transmissibility function:

$$G_1(s) = \frac{1}{(\tau s + 1)^2} \text{ where } \tau = 5.305 \text{ sec} \quad (3)$$

Note that this is based on the Bode's Plot [2] for which the break-off frequency is 0.03 Hz. Above 1.5 Hz, the transmissibility is much below the desired value.

3.2. CASE II

Using the properties of asymptotic nature of Bode's magnitude plot [2], the transfer function which will yield the transmissibility close to the desired function (Fig. 2) over the complete frequency spectrum can be shown to be as follows:

$$G_0(s) = \frac{K_0 (s^2 + 2\zeta\omega_{n1}s + \omega_{n1}^2) (s^2 + 2\zeta\omega_{n2}s + \omega_{n2}^2)}{(s^2 + 2\zeta\omega_{n3}s + \omega_{n3}^2) (s^2 + 2\zeta\omega_{n4}s + \omega_{n4}^2)} \quad (4)$$

where $\omega_{n1} = 1.5 * 2\pi$ (rad/sec), $\omega_{n2} = 3.0 * 2\pi$ (rad/sec), $\omega_{n3} = 0.03 * 2\pi$ (rad/sec), $\omega_{n4} = 15.0 * 2\pi$ (rad/sec), $\zeta = 0.707$ and K_0 is obtained such that

$$G_0(0) \approx 1 \quad (5)$$

Therefore,

$$K_0 \approx \frac{\omega_{n3}^2 \omega_{n4}^2}{\omega_{n1}^2 \omega_{n2}^2} \quad (6)$$

It is noted that due to numerical calculation error, $G_0(0)$ cannot be exactly identical to 1.0 in practice. From Fig. 1, the transmissibility effect is not crucial below 0.03 Hz. That is, the acceleration level of experiment module can be allowed to exceed the estimated space environmental acceleration to a certain extent. Nevertheless, K_0 will be chosen such that $G_0(0)$ is close to but less than 1.0.

4. Controller design

The control law is developed such that the desired transmissibility is achieved. Since the displacement of the experiment module relative to its support, $(y - x)$, and the absolute acceleration of the experiment module, (\ddot{y}) , can be directly measured in the space station, they are used as feedback signals. In order to appreciate the need for acceleration (\ddot{y}) feedback, only the relative displacement is used at first. The structure of the control system is shown in Fig. 4 where $d(s)$ is the extra disturbance which is assumed to be absent, and $H_j(s)$, $j = 1, 2$, represent the controller transfer functions for CASE I and CASE II, respectively.

For convenience, the following definitions are made.

Desired transmissibility functions

$$G_j(s) = \frac{K_j N_j(s)}{D_j(s)} \quad (7)$$

where K_j : D.C. gain of $G_j(s)$,

$N_j(s)$: Numerator polynomial of $G_j(s)$ with leading coefficient equal to 1.0,

$D_j(s)$: Denominator polynomial of $G_j(s)$ with leading coefficient equal to 1.0.

Note that $j = 1$ and $j = 2$ represent CASE I and CASE II, respectively.

Controller transfer function

$$H_j(s) = \frac{K_{Hj} N_{Hj}(s)}{D_{Hj}(s)} \quad (8)$$

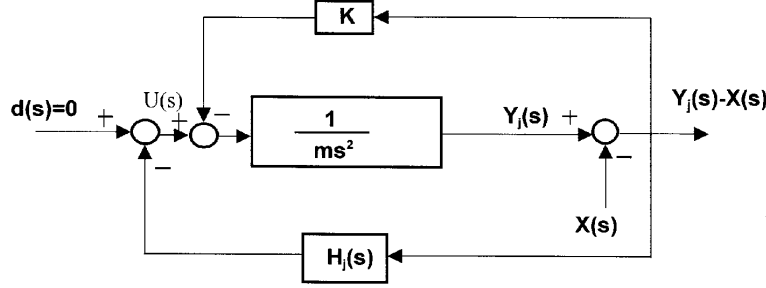


Fig. 4. Control system with relative displacement feedback.

where K_{H_j} , N_{H_j} , and D_{H_j} are defined in a manner similar to definitions of K_j , $N_j(s)$, and $D_j(s)$ in Eq. (7).

The controller transfer function that yields the desired transmissibility function is hence obtained as follows:

$$H_j(s) = \frac{K_j[ms^2 + k]N_j(s) - kD_j(s)}{D_j(s) - K_jN_j(s)} \quad (9)$$

where $j = 1, 2$. In order to get a proper controller transfer function, the degree of $[N_j(s)(ms^2 + k)]$ should not be greater than that of $D_j(s)$.

From Fig. 4, the relation between $Y_j(s)$ and $X(s)$ can be easily obtained. When the controller $H_j(s)$ in Eq. (9) is implemented via control structure of Fig. 4, the output response of the closed-loop system is found as follow:

$$Y_j(s) = \left[\frac{ms^2K_jN_j(s)}{ms^2D_j(s)} \right] X(s) \quad (10)$$

Since s^2 is a common factor between numerator and denominator, an undesired pole-zero cancellation does exist. Therefore, an inner-loop controller is added as shown in Fig. 5. The absolute acceleration of the experiment module is used as the feedback signal for the inner-loop controller $H_I(s)$ that is designed as follows:

$$H_I(s) = \frac{c_1}{s} + \frac{c_2}{s^2} \quad (11)$$

where c_1 and c_2 are positive numbers. It is noted that the implementation of transfer function $H_I(s)$ would require double integration of the acceleration signal.

When $H_I(s)$ is included to achieve the desired transmissibility function, the response of the modified control system becomes as follows:

$$Y_j(s) = \frac{[ms^2 + c_1s + c_2]}{[ms^2 + c_1s + c_2]} G_j(s) X(s) \quad (12)$$

Equation (12) implies a stable pole-zero cancellation. In the presence of the inner-loop, the outer-loop

controller is synthesized in terms of desired transmissibility function and system parameters.

$$H_j(s) = \frac{K_jN_j(s) [ms^2 + c_1s + (c_2 + k)] - kD_j(s)}{D_j(s) - K_jN_j(s)} \quad (13)$$

where $j = 1, 2$.

4.1. CASE I

The desired transmissibility is defined by Eq. (3). From Eq. (13),

$$H_1(s) = \frac{(m - k\tau^2)s^2 + (c_1 - 2k\tau)s + c_2}{\tau s(\tau s + 2)} \quad (14)$$

Note that if $c_2 = 0$,

$$H_1(s) = \frac{(m - k\tau^2)s + (c_1 - 2k\tau)}{\tau(\tau s + 2)} \quad (15)$$

and

$$Y_1(s) = \frac{(ms + c_1)}{(ms + c_1)} G_1(s) X(s) \quad (16)$$

Therefore, the common factor between numerator and denominator is $ms + c_1$, which is assured stable for any $c_1 > 0$.

4.2. CASE II

The desired transmissibility is defined by Eq. (4). In order to get a proper $H_2(s)$, a stable second-order factor is added in the denominator of Eq. (4). Hence, the desired transmissibility function is modified as follows:

$$G_2(s) = [K_2(s^2 + 13.33s + 88.83) (s^2 + 26.66s + 355.31)] / [(s + \alpha)^2 (s^2 + 0.267s + 0.036) (s^2 + 133.3s + 8883.00)] \quad (17)$$

where K_2 is chosen as $0.01013\alpha^2$ to assure $G_2(0) \approx 1.0$. From Eqs (13) and (17), $(D_2(s) - K_2N_2(s))$, which is the denominator of transfer function $H_2(s)$, can be expressed in terms of α .

$$\begin{aligned} D_2(s) - K_2N_2(s) &= s^6 + (2\alpha + 133.567)s^5 \\ &+ (0.98987\alpha^2 + 267.134\alpha + 8918.627)s^4 \\ &+ (133.16\alpha^2 + 17837.254\alpha + 2376.56)s^3 \\ &+ (8910.528\alpha^2 + 4753.12\alpha + 319.79)s^2 \\ &+ (2304.592\alpha^2 + 639.58\alpha)s + 0.063\alpha^2 \end{aligned} \quad (18)$$

Applying Routh-Hurwitz method [2], the condition on α for the stability of the controller transfer function $H_2(s)$ is ensured as long as α is positive. It is noted that in order to avoid numerical error that might cause instability of the designed controller if α is selected to be too close to zero, α should be conservatively chosen such as $\alpha \geq 0.5$.

For a special case,

$$\begin{aligned} k &= 0, \quad m = 8.640935 \text{ kg}, \\ c_1 &= 12.2183 \text{ N-sec/meter} \\ c_2 &= 8.640935 \text{ N/meter}, \\ \alpha &= 1,000 \text{ rad/sec}, \end{aligned}$$

Equation (14) yields

$$H_2(s) = \frac{K_{H_2}N_{H_2}(s)}{D_{H_2}(s)} \quad (19)$$

where

$$K_{H_2} = 87532.67155 \quad (20a)$$

$$\begin{aligned} N_{H_2}(s) &= s^6 + 41.40400209s^5 + 857.0637431s^4 \\ &+ 8274.99928s^3 + 42407.46884s^2 \\ &+ 51733.4838s + 31562.1873 \end{aligned} \quad (20b)$$

$$\begin{aligned} D_{H_2}(s) &= s^6 + 2133.567s^5 + 1265922.627s^4 \\ &+ 151001532.1s^2 + 8915281425s^2 \\ &+ 2305230891s + 63042.7 \end{aligned} \quad (20c)$$

The implementation of a high-order filter has been discussed by Blackburn [1] in the context of microgravity isolation technology.

5. Performance of the control system

The performance of the control systems designed on the basis of transmissibility functions $G_1(s)$ in Eq. (3) and $G_2(s)$ in Eq. (17) are compared with respect to following criteria: transmissibility, required control force and the stiffness of the closed-loop system. The inner loop controller transfer function $H_I(s)$ is taken to be identical for both cases such that the comparison of performance is persuasive. Constant parameters are $m = 8.640935 \text{ kg}$, $c_2 = 8.640935 \text{ N/meter}$. c_1 is chosen as $c_1 = 2\zeta'\sqrt{c_2/m}$, where ζ' is the damping ratio for the inner loop structure and will be assigned to be as 0.1 or 0.707.

Transmissibility

The controller of CASE I obviously leads to a much better isolation than what is required above 1.5 Hz. On the other hand, the controller of CASE II leads to the most tolerant transmissibility function and also has more flexibility for designers. For instance, if the design parameter α is chosen to be 1,000 rad/sec, the transmissibility almost exactly matches the required function. If α is chosen to be 1.0 rad/sec, the resulting isolation system is even more conservative than that in CASE I.

Required control forces

From Fig. 5, the control force from inner-loop controller, denoted by $U_j^I(s)$, can be straightforward calculated as follows:

$$U_j^I(s) = -H_I(s)[s^2Y_j(s)] \quad (21)$$

Similarly, the control force from the outer-loop controller, $U_j^O(s)$, is expressed in terms of $H_I(s)$.

$$U_j^O = -H_j(s)[Y_j(s) - X(s)] \quad (22)$$

The total control force is nothing but the sum of $U_j^I(s)$ and $U_j^O(s)$ and becomes

$$\begin{aligned} U_j(s) &= -[s^2H_I(s) + H_j(s)]Y_j(s) \\ &+ H_j(s)X(s) \end{aligned} \quad (23)$$

If all initial conditions are zeros, $Y_j(s)$ can be simply described as

$$Y_j(s) = G_j(s)X(s) \quad (24)$$

Substituting Eqs (12), (14) and (24) into Eq. (23),

$$U_j(s) = [(ms^2 + k)G_j(s) - k]X(s) \quad (25)$$

Equation (25) implies that the net control force is only a function of the input $X(s)$, system parameters,

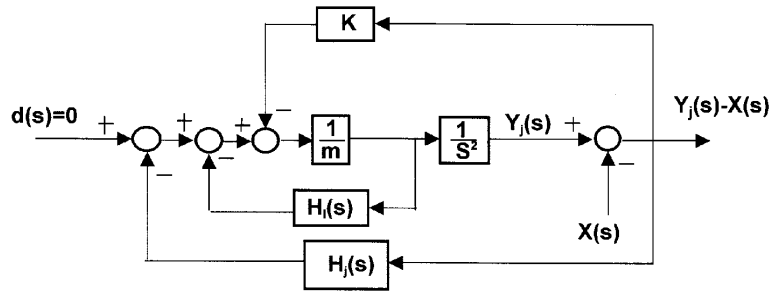


Fig. 5. Modified control system for microgravity isolation.

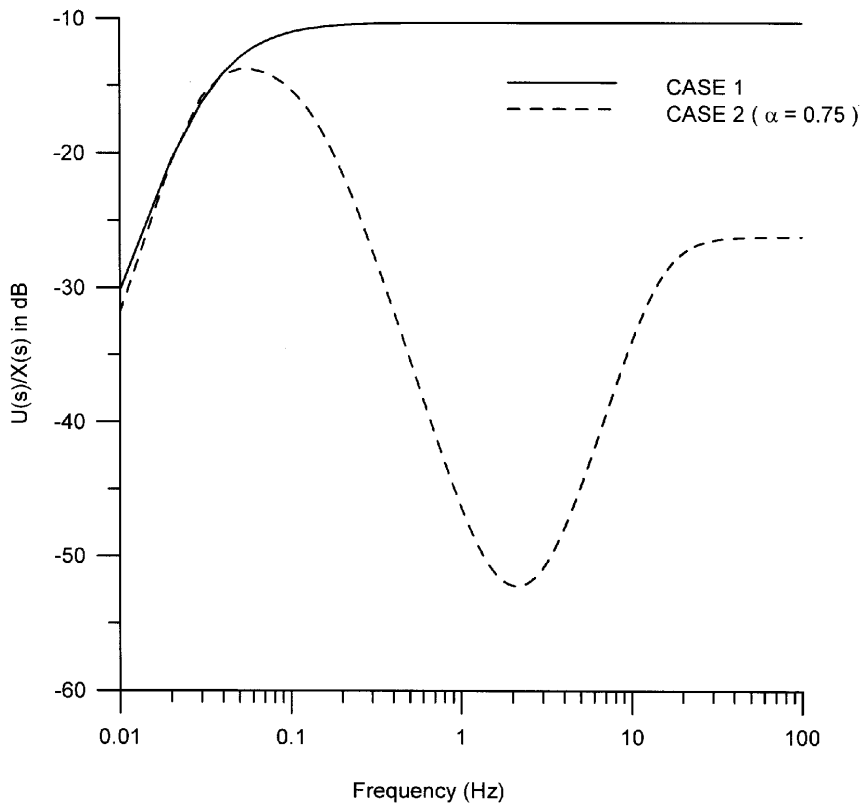
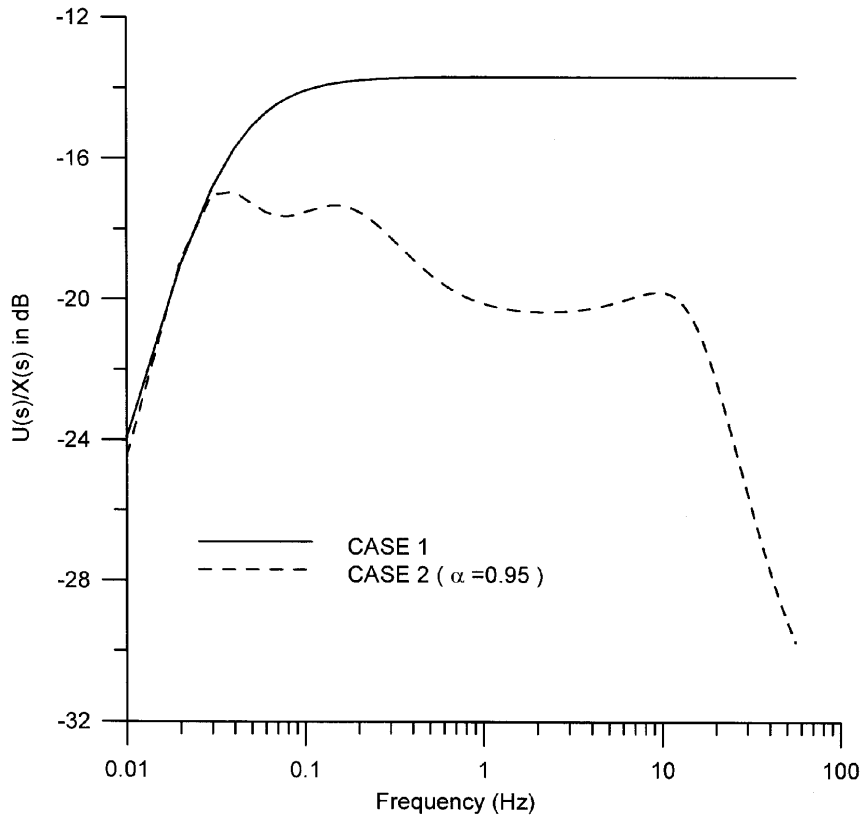


Fig. 6. Control force ($k = 0$).

m and k , and transfer function $G_j(s)$, i.e., $U_j(s)$ is independent of the inner-loop controller $H_I(s)$ or c_1 and c_2 . However, if initial conditions on $y_i(t)$ are not zeros, the control input will be a function of c_1 and c_2 . In fact, the inner-loop has been designed to counteract the effects of marginally stable pole-zero cancellations that exist only in the presence of non-zero initial conditions. When the system settles down in steady state in response to a sinusoidal displacement input $x(t)$, the amplitude and phase of $y_j(t)$ can be predicted by substituting $s = \omega i$ where $i = \sqrt{-1}$ into

Eq. (24). Therefore, Eq. (25) is valid to evaluate the magnitude of the control input in steady state. In other words, the input force is independent of c_1 and c_2 in steady state. The required net control inputs for both cases with $k = 0$ have been plotted in Fig. 6. Even if the stiffness k is increased to be 0.1 (N/m), the required control force of CASE II is usually less than that of CASE I by appropriately selecting the value of design parameter α (Fig. 7). That implies that the controller of CASE II leads to a relatively economical design and consumes less input energy.

Fig. 7. Control force ($k = 0.1$).

Equivalent stiffness of the closed-loop system

The experimental module may be excited by a direct force along with the base excitation. The effect of this disturbance will be smaller if the effective stiffness of the closed-loop system is higher. In order to examine the effective stiffness of the closed-loop system, the response of the system is determined when the direct excitation on the mass is a unit step function and there is no base excitation. The equation of motion in this case is as follows:

$$m\ddot{y}_i(t) + ky_j(t) = u_j^0(t) + u_j^I(t) + u_s(t) \quad (26)$$

where $u_j^0(t)$ and $u_j^I(t)$ are the control forces from the outer-loop and inner-loop controllers respectively and $u_s(t)$ is a unit step force applied at $t = 0$. Note that $y_1(t)$ and $y_2(t)$ represent the system responses in time for CASE I and CASE II, respectively. The steady-state values of $y_j(t)$ for both desired transmissibility functions (CASE I and CASE II) are obviously zeros by applying final value theorem. As a result, the maximum value of $y_j(t)$ is used as a measure of equivalent stiffness of the closed-loop system. The output

$y_j(t)$ is now examined for both aforementioned cases of desired transfer functions, i.e., CASE I and CASE II.

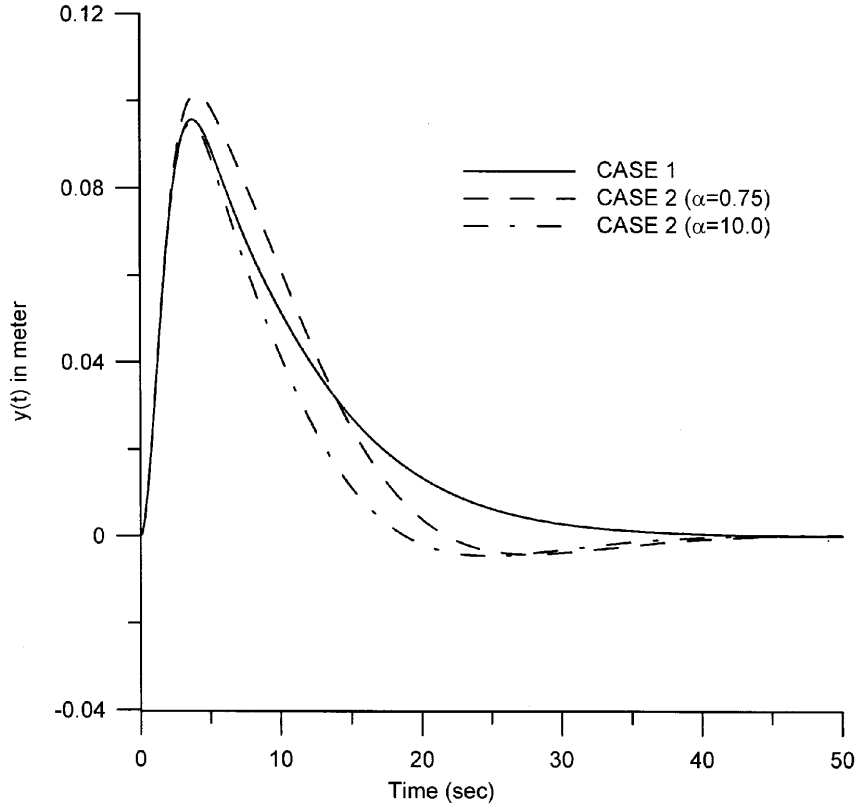
5.1. CASE I

The expression of $y_I(t)$ is easily found by Inverse Laplace Transform and Partial Fraction Method as follows:

$$my_I(t) = A_1 e^{-t/\tau} + A_2 t e^{-t/\tau} + A_3 e^{-\bar{c}_1 t/2} \sin(\beta t + \phi) \quad (27)$$

where $\beta = \sqrt{\bar{c}_2 - (\bar{c}_1/2)^2}$, $\bar{c}_1 = c_1/m$, and $\bar{c}_2 = c_3/m$. The expressions A_1, A_2, A_3 and ϕ are available in Tsai and Sinha [15].

For numerical evaluation on the closed-loop system stiffness, in Figs 8 and 9, the value of c_1 in each case has been chosen such that the damping ratio of the system with inner loop, ζ' , is 0.707, i.e., $c_1 = 1.414\sqrt{c_2/m}$ and 0.1, i.e., $c_1 = 0.2\sqrt{c_2/m}$ for a tenth unit-step excitation. It is found [15] that A_1 and A_3 are the dominating terms in the step response. Hence the maximum value of $y_j(t)$, used as a measure of effective

Fig. 8. Step response ($\zeta = 0.707$).

closed-loop system stiffness, is primarily governed by A_1 and A_3 which are due to factors $(\tau s + 1)^2$ and $(ms^2 + c_1s + c_2)$.

5.2. CASE II

The desired transmissibility is defined by Eq. (18). The unit step response is hence obtained as follows:

$$\begin{aligned}
 my_2(t) = & B_0 + B_1e^{-\alpha t} + B_2te^{-\alpha t} \\
 & + B_3e^{-0.1335t} \sin(\beta_3^t + \varphi_1) \\
 & + B_4e^{-66.65t} \sin(\beta_4t + \varphi_2) \\
 & + B_5e^{-\bar{c}_1t/2} \sin(\beta_5t + \varphi_3)
 \end{aligned} \quad (28)$$

where

$$\beta_3 = 0.1348 \text{ (rad/sec)}$$

$$\beta_4 = 94.0727 \text{ (rad/sec)}$$

$$\beta_5 = \sqrt{\bar{c}_2 - 0.25\bar{c}_1} \text{ (rad/sec)}$$

The expressions of $(B_0 - B_5)$ and $(\varphi_1 - \varphi_3)$ can be found in Tsai and Sinha [15]. Similarly, B_3 and B_5 are

the dominating terms which are due to the factors $(s^2 + 0.267s + 0.036)$ and $(ms^2 + c_1s + c_2)$, respectively.

In summary, dominating factors $(5.305s + 1)^2$ and $(s^2 + 5.305s + 0.036)$ represent terms with the lowest break-off frequency at 0.03 Hz in desired transfer functions for CASE I and CASE II, respectively. And the contribution of the inner loop $(ms^2 + c_1s + c_2)$ remains significant in both cases. Therefore, the equivalent closed-loop system stiffnesses (maximum of $y_j(t)$) are almost identical for both cases. Nevertheless, by selecting design parameter, α , the settle time of CASE II can be always shorter than that of CASE I (Figs 8 and 9).

6. Conclusions and future works

The control system has been developed to achieve the desired transmissibility represented by Eq. (18). This transfer function corresponds to the transmissibility shown in Fig. 2. The structure of the control system is shown in Fig. 5. The inner-loop controller transfer function $H_I(s)$ for the acceleration feedback loop is

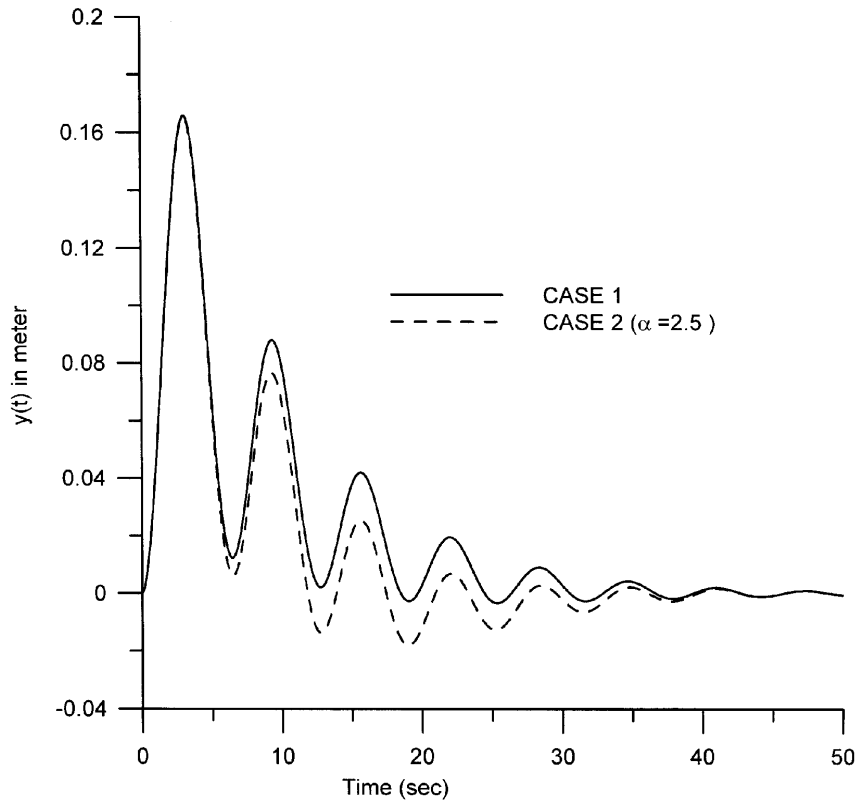


Fig. 9. Step response ($\zeta = 0.1$).

chosen to avoid undesired pole-zero cancellations. The controller transfer function $H_I(s)$ for relative displacement feedback is determined such that the resulting transmissibility equals to that given by Eq. (18). The factor $(s + \alpha)^2$ has been introduced in the denominator of Eq. (18) to ensure that $H_j(s)$ is proper. Applying Routh-Hurwitz method, a condition on α has been determined for stability assurance of inner-loop controller, $H_j(s)$. The transmissibility represented by Eq. (18) matches exactly with the specified transmissibility given in Fig. 2 by selecting large positive values of design parameter, α . As α decreases, the transmissibility becomes more and more conservative and eventually even less than that of CASE I. Meanwhile, the control cost of CASE II is always much less than that of CASE I as long as α remains below a certain positive value. It has been found that the equivalent closed-loop stiffness is primarily governed by $H_I(s)$ and the lowest break-off frequency in the desired transmissibility function. Although the control system of CASE II does not have evident superior equivalent closed-loop stiffness, its settle time is shorter than that of CASE I by proper choice of α .

Vibration isolation for microgravity experiments is indeed a challenging control problem. Although the modern optimal and robust control methodologies, to ensure stability and performance of the inherently multivariable system with uncertainties and nonlinearities, are beyond the scope of this report, they will definitely be the most interesting and important research issues in future works. In fact, several reports for the investigations and studies of these areas are already available (e.g. [4,8]). In addition, the actuator for microgravity isolation has to be chosen and designed practically capable of making quick response with respect to the base motion. Lastly, the actuator's bandwidth, high-frequency responses of experiment modules, different patterns of acceleration-input levels and various experiment facilities could be taken into consideration as well in future works.

References

- [1] J. Blackburn, New Inertial Actuator provides Isolation and Stabilization in Microgravity Conditions, presented at the *International Workshop on Vibration Isolation Technology for*

- Microgravity Science Applications*, NASA Lewis Research Center, NASA CP 10094, 1991.
- [2] R.C. Dorf, *Modern Control Systems*, Addison-Wesley, reading, Mass., USA, 1986.
- [3] R.C. Fenn, J.R. Downer, V. Gondhalekar and B.G. Johnson, An Active Magnetic Suspension For Space-Based Microgravity Vibration Isolation, *Active Noise and Vibration Control*, (Vol. 8), ASME NCA, 1990, pp. 49–56.
- [4] I.J. Fialho, Control Design for the Active Rack Isolation System, Proc. 2000 American Control Conference, Chicago, 2000, pp. 2082–2087.
- [5] C.M. Grodsinsky and G.V. Brown, *Low Frequency Vibration Isolation Technology for Microgravity Space Experiments*, NASA TM-101448, 1989.
- [6] C.M. Grodsinsky, Vibration Isolation Technology Development to Demonstration, Presented at the *International Workshop on Vibration Isolation Technology for Microgravity Science Application*, NASA Lewis Research Center, NASA CP 10094, 1991.
- [7] C.M. Grodsinsky and M.S. Whorton, Survey of Active Vibration Isolation Systems for Microgravity Applications, *Journal of Spacecraft and Rockets* **37**(50) (2000), 586–596.
- [8] R.D. Hampton, C.R. Knospe and C.M. Grodsinsky, Microgravity Isolation System Design: A Modern Control Synthesis Framework, *Journal of Spacecraft and Rockets* **33**(1) (1996), 101–109.
- [9] D.I. Jones et al., *Microgravity Isolation Mount*, European Space Agency, Final Report No. 1755/85, 1987.
- [10] D.I. Jones, A.R. Owens and R.G. Owens, A Microgravity Isolation Mount, *Acta Astronautica* **15**(6/7) (1987), 441–448.
- [11] D.I. Jones, A.R. Owens and R.G. Owens, A Microgravity Facility for In-orbit Experiment, *Active Noise and Vibration Control*, (Vol. 8), ASME NCA, 1990, pp. 67–73.
- [12] D.S. Stampleman and A.H. Flotow, Microgravity Isolation Mounts Based Upon Piezoelectric Film, *Active Noise and Vibration Control*, (Vol. 8), ASME NCA, 1990, pp. 57–65.
- [13] A. Sinha, C.K. Kao and C. Grodsinsky, A New Approach to Controller Design for Microgravity Isolation System, *Acta Astronautica* **21**(11/12) (1990), 771–775.
- [14] A. Sinha and Y.-P. Wang, Digital Control Algorithms for Microgravity Isolation Systems, *ASME Journal of Vibration and Acoustics* **115**(3) (1993), 256–263.
- [15] N.-C. Tsai and A. Sinha, Effects of Transmissibility on Performance and Design of Desired Transfer Function for Microgravity Isolation Systems, *Proceedings of 1995 ASME Design Engineering Technical Conference*, (Vol. 3), Part C, Vibration Control, Analysis and Identification, 1995, pp. 89–96.
- [16] R.G. Owen, D.I. Jones and A.R. Owens, Mechanical Design and Simulation of a Microgravity Isolation Mount for Columbus, *Journal of Spacecraft and Rockets* **30** (1993), 502–508.
- [17] G.E. Waranka, C. Radcliffe and A.H. Flotow, eds, *Active Noise and Vibration Control*, (Vol. 8), ASME NCA, 1990.



Hindawi

Submit your manuscripts at
<http://www.hindawi.com>

